Hindawi Publishing Corporation
Journal of Nanomaterials
Volume 2013, Article ID 154874, 9 pages
http://dx.doi.org/10.1155/2013/154874

Research Article

Polyethylene/Clay Nanocomposites Produced by *In Situ* Polymerization with Zirconocene/MAO Catalyst

Pimpatima Panupakorn,[1] Ekrachan Chaichana,[2] Piyasan Praserthdam,[1] and Bunjerd Jongsomjit[1]

[1] *Center of Excellence on Catalysis and Catalytic Reaction Engineering, Department of Chemical Engineering, Faculty of Engineering, Chulalongkorn University, Bangkok 10330, Thailand*
[2] *Chemistry Program, Faculty of Science and Technology, Nakhon Pathom Rajabhat University, Nakhon Pathom 73000, Thailand*

Correspondence should be addressed to Bunjerd Jongsomjit; bunjerd.j@chula.ac.th

Received 14 June 2013; Revised 25 July 2013; Accepted 25 July 2013

Academic Editor: Shanfeng Wang

Two commercial nanoclays were used here as catalytic fillers for production of polyethylene (PE) and linear low-density polyethylene (LLDPE) nanocomposites via *in situ* polymerization with zirconocene/MAO catalyst. It was found that both types of nanoclays designated as clay A and clay B can improve thermal stability to the host polymers as observed from a thermal gravimetric analysis (TGA). The distribution of the clays inside the polymer matrices appeared good due to the *in situ* polymerization system into which the clays were introduced during the polymer forming reaction. Upon investigating the clays by X-ray diffractometer (XRD) and Fourier transform infrared spectroscopy (FTIR), it was observed that the crucial differences between the two clays are the crystallite sizes (A < B) and the amounts of amine group (A < B). The higher amount of amine group in clay B was supposed to be a major reason for the lower catalytic activity of the polymerization systems compared to clay A resulting from its deactivating effect on zirconocene catalyst. However, for both clays, increasing their contents in the polymerization systems reduced the catalytic activity due to the higher steric hindrance occurring.

1. Introduction

During the growth of polyolefin production, polyethylene (PE) is considered as one of the most widely used synthetic polymer with the annual production approximately 80 million metric tons [1]. This is due to its unique properties such as light weight, high chemical resistance, and low dielectric constant. However, the polyethylene properties have some restrictions on its use. It does not have enough stiffness, has low gas permeability, and can easily catch fire. Therefore, improving the polyethylene properties is important. Addition of additives or fillers can improve polyethylene properties such as mechanical property, thermal property, barrier property, and flame resistant. Due to the advantage of nanotechnology nowadays, nanoscale materials have been used as fillers instead of conventional microscale materials and also provide better properties. The polymers with the addition of nanofiller can be designated as polymer nanocomposites. The final properties of polymer nanocomposites depend strongly on the properties of the filler. Different types of nanofillers have been used in the production of polymer nanocomposites including organic nanofiller such as cellulose and inorganic nanofiller such as carbon nanotube (CNT) [2, 3], silica (SiO_2) [4], alumina (Al_2O_3) [5], and clay [6, 7]. Using nanoclay as a filler is of interest for nanocomposite production due to ready availability and low cost. Zhao et al. [6] studied the properties of PE/clay nanocomposites, which were prepared by melt mixing and found that the mechanical and flammability properties of the polymers improved with the clay addition. Huang et al. [7] studied the thermal stability and fire behavior of LDPE/clay nanocomposites, which were prepared by melt mixing, and observed the improved thermal stability and flame retardant. Besides the nature of fillers and their content in the product, the adhesion between matrix and filler and the aspect ratio of the filler are also the key factors in the improvement of the polymer final properties [8]. The platelet nanoclay is one of the high aspect ratio fillers, therefore receiving considerable attention. For enhancing the adhesion between

two phases, modification of nanoclay with appropriate agent is usually used for this purpose. Hakim et al. [9] investigated clay nanoplatelets treated (modified) with ammonia and dodecylamine at different conditions in the *in situ* ethylene polymerization system with metallocene catalyst (Cp_2ZrCl_2). It was found that the treated clays provided the higher catalytic activity than the untreated clays. However, the modifiers sometimes deteriorate the polymerization systems particularly for the *in situ* polymerization systems into which the modified fillers were introduced during the polymer growing process [10].

In this study, the two commercial nanoclays completely modified with different amounts of amine group were investigated to compare their roles in the *in situ* polymerization with MAO/metallocene catalysts for the production of PE/clay composite and LLDPE/clay composite. The nature of both clays was characterized using Fourier transform infrared spectroscopy (FTIR) and X-ray diffraction analysis (XRD). The effect of clay natures and loadings on the nanocomposite properties and the catalytic activity of polymerization systems were studied by nuclear magnetic resonance (^{13}C NMR), scanning electron microscopy (SEM), and so forth.

2. Experimental

2.1. Materials. All chemicals and polymerization were performed under an argon atmosphere using a glove box and/or Schlenk techniques. Nanoclays (montmorillonite, MMT containing different amounts of amine group) were donated by Thai Nippon Chemical Industry Co., Ltd., Thailand. Toluene was dried over dehydrated $CaCl_2$ and distilled over sodium/benzophenone before use. The *rac*-ethylenebis (indenyl) zirconium dichloride (*rac*-Et$[Ind]_2ZrCl_2$) was obtained from Aldrich Chemical Company, Inc. Methylaluminoxane (MAO) in hexane was donated by Tosoh (Akzo, Japan). Ultrahigh purity argon was purchased from Thai Industrial Gas Co., Ltd. And was further purified by passing it through columns that were packed with BASF catalyst R3-11G (molecular-sieved to 3 Å), sodium hydroxide (NaOH), and phosphorus pentoxide (P_2O_5) to remove traces of oxygen and moisture. Ethylene gas (99.96%) was donated by the National Petrochemical Co., Ltd., Thailand. 1-Hexene (99%, d = 0.673 g/mL) and hydrochloric acid (HCl, fuming 36.7%) were purchased from Aldrich Chemical Company, Inc. Methanol (commercial grade) was purchased from SR Lab Co., Ltd.

2.2. Treatment of Nanoclay. The nanoclay (clay A or clay B) was heated at 150°C for 2 h and then heated at 150°C for 2 h under argon atmosphere.

2.3. Preparation of Catalyst. In the glove box, *rac*-Et$(Ind)_2ZrCl_2$ 0.0083 g (1.98×10^{-5} moles) was added in 20 mL of toluene solution and stirred at room temperature at least 30 min or until giving yellow transparent solution.

2.4. In Situ Polymerization. In situ polymerization was conducted under argon atmosphere using Schlenk techniques and/or glove box. It was carried out in a 100 mL semibatch stainless steel autoclave reactor equipped with a magnetic stirrer. The desired amount of nanoclay (5, 10, 20, and 40 wt%) as support and methylaluminoxane (MAO) 1.1 mL ($[Al]_{MAO}/[Zr] = 1135$) were mixed and stirred for 30 min aging at room temperature. Then, catalyst solution 1.5 mL [$Et(Ind)_2ZrCl_2$ 5×10^{-5} M] along with toluene (to make total volume of 30 mL) was put into the reactor. Then, ethylene was fed into the reactor equipped with pressure gauge. After all ethylene was consumed (6 psi from pressure gauge), the reaction was terminated by addition of acidic methanol and stirred overnight. After filtration and dried at room temperature, polyethylene/clay nanocomposite is obtained. For copolymerization, 1-hexene as comonomer (1 : 0.5 of ethylene : 1-hexene ratio) was also put into the reactor.

2.5. Characterization

2.5.1. Characterization of Nanoclay

X-Ray Diffraction Analysis (XRD). The crystallite structure of nanoclay was investigated by X-ray diffractometer SIEMENS D-5000 with Cu K_α ($\lambda = 1.54439$ Å). The range of detection $2\theta = 10$–80°.

Thermal Gravimetric Analysis (TGA). TGA was used to determine the thermal stability of clay in terms of weight loss. The sample was analyzed by TGA, PerkinElmer Thermal Analysis Diamond TG/DTA. The analysis was preceded under nitrogen atmosphere at gas flow rate of 100 mL/min. The sample was heated from 25°C to 300°C at a constant rate of 10°C/min and then cooled naturally.

Fourier Transform Infrared Spectroscopy (FTIR). FTIR was used to identify specific structural characteristics (e.g., functional group or molecular structure) of nanoclay using Nicolet 6700 FTIR.

2.5.2. Characterization of Nanocomposites

Small Angle X-Ray Diffraction Analysis (SAXRD). SAXRD was used to identify the sample by comparison with reference sample and to determine the interlayer spacing of nanoclay in polymer matrix. XRD patterns of polyethylene/clay nanocomposites were observed using Bruker AXS Model D8 Discover X-ray diffractometer with VANTEC-1 Detector (Super Speed Detector) 46 connected to a personal computer for full control of the XRD analyzer. The observation was preceded by using Cu radiation measurement, 2θ range of detection is 1–10 degree, and increment is 0.02 degree/step.

Thermal Gravimetric Analysis (TGA). TGA was used to determine the thermal stability in terms of weight percent in the sample as a function of temperature. PE/clay nanocomposites were analyzed by TGA, PerkinElmer Thermal Analysis Diamond TG/DTA. The analysis was performed under nitrogen atmosphere at gas flow rate of 100 mL/min. The sample was heated from 50°C to 600°C at a constant rate of 10°C/min and then cooled naturally.

Differential Scanning Calorimetry (DSC). The melting temperature (T_m) was determined by a Perkin-Elmer diamond DSC. The analysis was proceeded at the heating rate of 20°C/min in the temperature range of 50–150°C under N_2 atmosphere. The heating cycle was run twice. In the first scan, the samples were heated and then cooled to room temperature. In the second scan, the samples were reheated at the same rate, but only the results of the second scan were reported because the first scan was influenced by the mechanical and thermal history of the samples.

Nuclear Magnetic Resonance (^{13}C NMR). ^{13}C NMR was used to evaluate the percent insertion of comonomer in the copolymer. For sample preparation, LLDPE/clay nanocomposite was dissolved in the mixture of 1,2,4-trichlorobenzene and chloroform-d (internal locking solvent) and then heated until it became a clear solution. The ^{13}C NMR spectra were recorded at 110°C using JEOL JNM-A500 operating at 125 MHz.

Scanning Electron Microscopy (SEM). SEM was used to observe the morphology of polymer nanocomposites. The sample was analyzed by JEOL JSM-6400 scanning electron microscopy. The nanocomposite samples were mounted on a stub with double-sided adhesive tape and coated with a thin layer of gold prior to observation.

3. Results and Discussion

3.1. Characterization of Nanoclay

3.1.1. Size and Composition. Figure 1 shows the XRD patterns of nanoclay. The sizes of nanoclay were investigated by X-ray diffraction (XRD). From Debye-Scherrer formula [6], it was confirmed that the average crystallite sizes of clay A and clay B are ca. 4 and 7 nm (using the XRD peak at 22°), respectively.

Both clay XRD patterns present the peaks in the positions (2θ) of 20, 22, 26.5, and 36°, corresponding to montmorillonite (MMT) crystalline structure [11]. The position at 10.1° corresponds to illite clay mineral, which is a phyllosilicate or layered aluminosilicate. This indicates that these nanoclays are mixed-layer montmorillonite/illite, which is composed of two discrete species: one is montmorillonite having low interlayer charge with hydrated interlayers by at least two layers of water molecules; the second species is illite with dehydrated interlayers.

3.1.2. Functional Group. The functional groups of two types of nanoclay were compared by FTIR spectra. The FTIR spectra are shown in Figure 2. It was found that the wavenumbers of obtained peaks are not different and the absorbances are also rather equal. FTIR spectra show the main peaks at 1000, 2850, and 2900 cm^{-1} wavenumbers, which are corresponding to alkene (=C–H bending), CH stretching vibrations (CH_2), and alkane (C–H stretch), respectively, [12]. The peak between 3,300 and 3,500 cm^{-1} was considered as amine (N–H stretch) [12]. The absorbance peak of clay A is lower than clay B. This indicates that amine compound in clay A is less than clay B. It may be due to the different amounts of amine salts in the surface of the clay. Moreover, it was possible that clay A and clay B were modified by the different kinds of amine salts, which include primary, secondary, or tertiary amine salt.

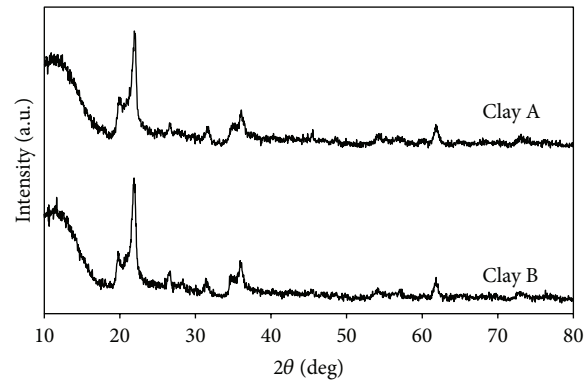

Figure 1: XRD patterns of nanoclay.

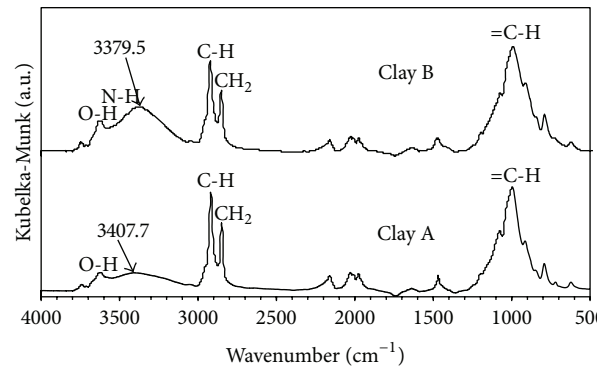

Figure 2: FTIR spectra of clay A and clay B.

3.1.3. Thermal Stability. Thermal stability of nanoclay in nitrogen atmosphere can be observed from Figure 3, which indicates that clay A is more stable than clay B at a temperature lower 300°C. The thermal stabilities were evaluated in terms of 10% weight-loss temperatures (T_d10). T_d10 of clay A is higher than clay B, which are 273 and 227°C, respectively. This difference in thermal stability was due to different compositions of these nanoclays. In general, the unmodified clay (such as Na^+-Montmorillonite) has weight loss at ca. 100°C due to the presence of moisture in the interlayer between clay platelets. However, for clay A, the weight loss at ca. 100°C was not observed. This indicates that the surface of the clay platelets had been modified with an organic modifier (alkyl ammonium salt), conveying hydrophobic properties to the hydrophilic clay. From 200°C, the weight loss was observed on clay A due to the decomposition of the alkyl amine salt [13]. In clay B, the first weight loss was observed at 90°C. It is attributed to the decomposition of the remaining moisture in this clay. Above 200°C, clay B exhibited lower stability than clay A. The alteration of thermal stability may be derived from the various kinds and amounts of amine salts between the two clays.

Table 1: Catalytic activities of polymerization systems with various fillers.

Run	Polymer	Amount of clay (wt%)		Yield[a] (g)	Activity[b] (kg pol./mol Zr·h)
		Clay A	Clay B		
1	PE	—	—	1.3643	17,588
2		5	—	0.6622	12,851
3		10	—	0.7083	8,730
4		20	—	0.5894	6,869
5		40	—	0	0
6		—	10	0.7937	8,007
7		—	20	0.2906	5,440
8		—	40	0	0
9	LLDPE	—	—	1.3087	35,534
10		5	—	1.1045	20,036
11		10	—	1.2241	12,143
12		20	—	0.3998	5,578
13		40	—	0	0

[a]The polymer yield was limited by the amount of ethylene fed (0.018 mol). The molar ratio of ethylene: comonomer was 2 : 1.

[b]Activities were measured at polymerization temperature of 70°C, [ethylene] = 0.018 mol, $[Al]_{MAO}/[Zr]_{cat}$ = 1135 in toluene with total volume = 30 mL, $[Zr]_{cat} = 5 \times 10^{-5}$ molar and mixing time of MAO and nanoclay was 30 min.

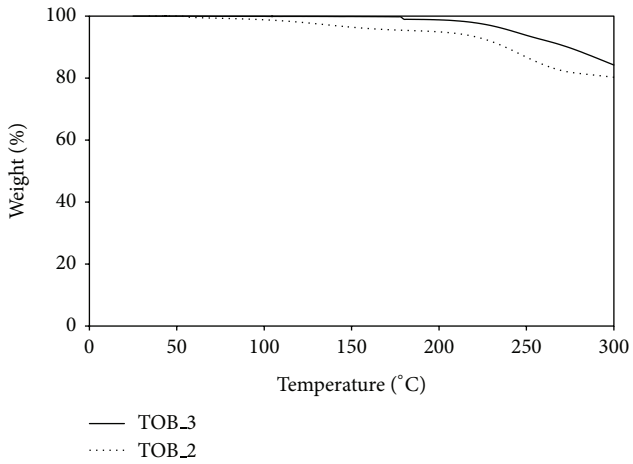

Figure 3: TGA curves of nanoclays (clay A: TOB_3 and clay B: TOB_2).

3.2. Ethylene Polymerization. The effect of the types of nanoclay on the activity of metallocene catalyst as shown in Table 1 indicates that the polymerization system with clay A exhibits higher catalytic activity than that with clay B at the same loading. This is consistent with the higher amount of amine group in clay B, which may deactivate zirconocene catalyst [10, 14]. Therefore, clay A is more appropriate to use as nanofiller for catalytic aspect. It is also observed that the catalytic activity of the homogeneous systems (runs 1 and 9) is higher than that of the heterogeneous (with clays) systems (runs 2–8 and 10–13). The reduction of the catalytic activity for the heterogeneous systems can be attributed to (1) the generation of catalyst active sites with lower propagation rates due to interactions with the clay surface, and (2) restrictions of the monomer access to the catalyst active sites due to the presence of the clays, hindering the chain propagation [15]. In addition, the catalytic activity tended to decrease with the increase of the nanoclay content. This is because the drawbacks of the heterogeneous system as mentioned above were more pronounced when the higher amounts of nanoclay were present in the systems. The deactivating effect of the amine group on the zirconocene catalyst is also another reason for the decrease of catalytic activity. When increasing the amount of nanoclay to 40 wt%, it did not even produce polyethylene due to the more adverse effect from the nanoclays.

3.3. Characterization of Nanocomposites. It was because clay A provided the higher catalytic activity than clay B, thus it was more appropriate to be used as the catalytic filler. Therefore, in this characterization of nanocomposites, only clay A-filled nanocomposites were investigated and compared with the pure polymers.

3.3.1. Dispersion of Nanoclay. The small angle X-ray diffraction (SAXRD) patterns of nanoclay (clay A), pure PE, and PE/clay nanocomposites are shown in Figure 4. The SAXRD patterns for clay A provide diffraction peaks at 2 = 2.3 and 4.7°, whereas the pure PE did not exhibit the diffraction peak at 2 = 1–10° range. The diffraction peaks of all nanocomposites were also not observed. The peaks at about 2 = 2.3 and 4.7° of clay were not in the nanocomposites suggesting that high dispersion of nanoclay throughout polyethylene matrix was obtained [16]. This exfoliated degree dispersion of nanoclay may be due to direct mixing process. The methylaluminoxane (MAO) added during the clay treatment step is expected to react with hydroxyl group on clay surface. After that, the zirconocene catalyst added during catalyst supported step was intercalated between the clay platelets, where the zirconocene catalyst was reacted with MAO-treated clay and modifier, creating covalent bond that helps to avoid catalyst leaching during the polymerization. Thus, it is the cause

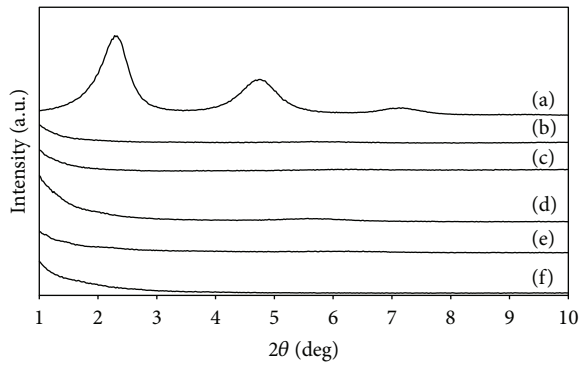

Figure 4: SAXRD patterns of (a) clay A, (b) LLDPE/clay 10 wt%, (c) LLDPE/clay 5 wt%, (d) PE/clay 10 wt%, (e) PE/clay 5 wt%, and (f) pure PE.

of well dispersion of nanoclay in the polyethylene matrix [17]. Exfoliation became possible through a strong interaction between the polyethylene chains and the clay surface [18].

3.3.2. Thermal Stability. Figure 5 shows TGA and DTG curves of pure PE and PE/clay nanocomposites. It is used to describe thermal stability of PE/clay nanocomposites. At temperature range between 200 and 350°C, PE/clay nanocomposite degraded slower than pure PE observed from the lower weight loss percentage, whereas the nanocomposite with 20 wt% of clay loading exhibited faster degradation. The weight loss at this temperature range is related mainly to the organic surface modifier degradation and also the degradation of remained MAO that cannot participate in the polymerizations [9]. In effect, the nanocomposite with 20 wt% of clay loading, which naturally has the highest content of the organic surface modifiers among all the samples and also has the highest content of the remained inactive MAO due to the lowest catalytic activity, thus degraded fastest in this temperature range. For the nanocomposites with 5% and 10 wt% of clay loadings, they degraded slower than the pure polymer due to the major effect of barrier properties induced by the nanoclays that hindered heat transfer throughout the nanocomposites [19]. At the temperature above 400°C, the weight loss of the polymer contributes to polymeric chain degradation. It was found that the nanocomposite with 5 wt% of clay loading still exhibited better thermal stability than the pure polymer and other nanocomposite samples. The lower thermal stabilities of the nanocomposites with the higher loadings (10 and 20 wt%) compared to the pure polymer are attributed to the presence of more acidic sites originating from the Hoffman degradation of the organic surface modifiers, which catalyze the polymer chain degradation [20, 21]. Therefore, it can be concluded from the TGA result that the introduction of clay into the polymers not exceeding 5 wt% can enhance their thermal stability, but the excess of clay (from 10 wt%) can reduce the thermal stability of the polymer. For DTG curve, the maximum decomposition temperatures were observed. The maximum decomposition temperatures of pure PE, PE/clay 5, PE/clay 10, and PE/clay 20 are 463, 481, 452, and 449°C,

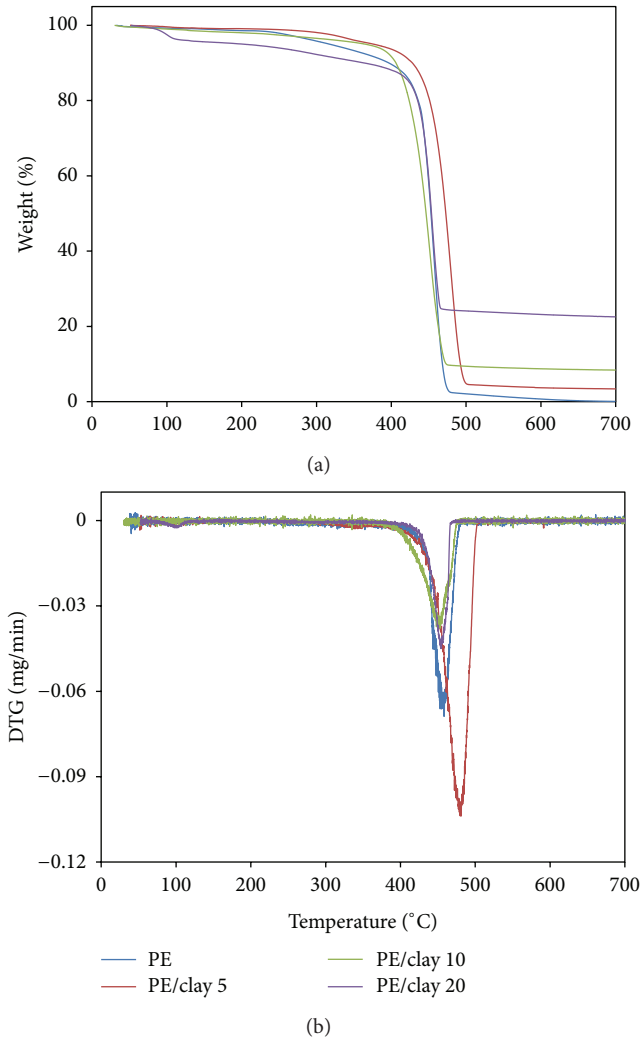

Figure 5: TGA and DTG curves of PE and PE/clay nanocomposites.

respectively. It can be observed that from 10 wt% to 20 wt% of clay content, the maximum decomposition temperatures of the nanocomposites decreased with increasing the clay content. This result is attributed to an increase of the acidic sites with increasing the organic surface modifiers (from clays), which accelerated the polymer degradation.

The thermal properties of LLDPE and its nanocomposites investigated by TGA and DTG are shown in Figure 6. It was found that the maximum decomposition temperatures of pure LLDPE, LLDPE/clay 5, LLDPE/clay 10, and LLDPE/clay 20 are 463, 463, 465, and 442°C, respectively. This thermal behavior of LLDPE slightly differed from that of PE probably due to the difference in molecular structure and crystallinity between two polymers, then being affected by the clay differently.

3.3.3. Crystallization Behavior. Table 2 shows the melting temperature, crystallinity, and 1-hexene insertion (obtained from ^{13}C NMR spectrum as shown in Figure 7) of pure PE, pure LLDPE, and the nanocomposites. It can be observed that

Table 2: Melting temperature, crystallinity, and 1-hexene (comonomer) insertion of the polymers and polymer nanocomposites.

Run	Polymer	Amount of clay A (wt%)	T_m[a] (°C)	X_c[b] (%)	1-Hexene insertion[c] (%)
1	PE	—	134	51	—
2		5	134	57	—
3		10	132	51	—
4		20	132	44	—
9	LLDPE	—	114	3	32.2
10		5	n/a[d]	n/a	29.6
11		10	132	28	15.8
12		20	108	23	5.2

[a]Melting temperature (T_m) was obtained from DSC measurement.
[b]Crystallinity (X_c) was calculated based on DSC results.
[c]1-Hexene insertion was obtained from ^{13}C-NMR spectrum equalling to [HHH] + [HHE] + [EHE].
[d]Not detected.

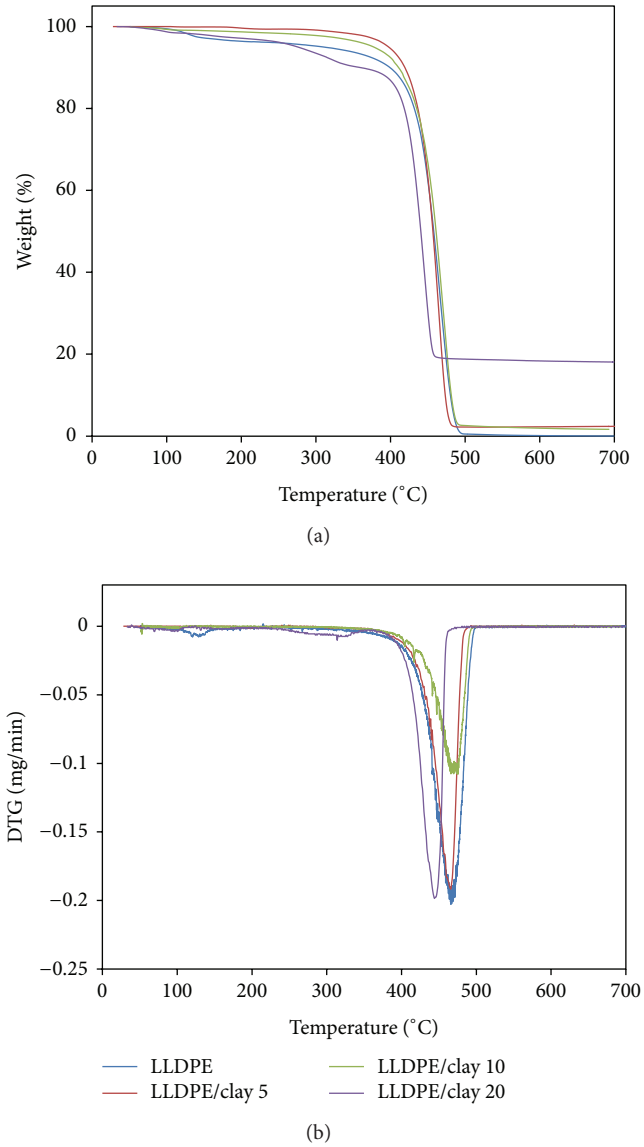

Figure 6: TGA and DTG curves of LLDPE and LLDPE/clay nanocomposites.

there was no significant change in the melting temperature of PE with the addition of nanoclay in homopolymerization system. However, it is seen that PE/clay nanocomposites with various clay loadings are different in the crystallinity. Adding 5 wt% of clay in the composite presents an increase in crystallinity. This suggests that small amount of clay acting as heterophase crystal nucleation agent in the polymer metrix [18]. However, the crystallinities of PE/clay nanocomposites decreased by increasing the amounts of nanoclay to 10 and 20 wt%. This may be due to large amounts of clay particles locating themselves in the interlamellar spaces, leaving a little room for additional crystallization. Thus, clay particle may hinder the formation of crystalline phase of PE and present a decrease in crystallinity [18]. For the copolymerization system in which 1-hexene was used as a comonomer, no melting temperature was found for LLDPE with 5 wt% of clay (run 9). It may be due to too much insertion of 1-hexene comonomer (over 30%), which poses the large molecular structure, and also the effect of clay that prevents the crystallization process inside the polymer. This contrasts with the pure LLDPE (run 8) which only the high comonomer insertion occurred without the presence of clay. Therefore, its crystallinity still appeared. The melting temperatures and the crystallinities were observed in the case of LLDPE with 10 and 20 wt% of clay (runs 11 and 12). It may be due to a decrease of comonomer insertion resulting from the higher content of clay that brought the crystallinity back to the nanocomposites. The higher content of the clay in the polymerization system could lead to less space for monomer (ethylene) or comonomer (1-hexene) attacking into the catalyst active sites. On account of this phenomenon, 1-hexene molecules which are larger than ethylene molecules then have the lower ability to attack the active sites when the clay content is higher. Therefore, the insertion of the 1-hexene decreased by increasing the amount of the clay.

3.3.4. Morphology. The SEM micrographs of the PE and PE/clay nanocomposites are shown in Figure 8. It can be seen that no agglomerated particles leaching out from the polymer matrix were clearly observed. This suggests good distribution

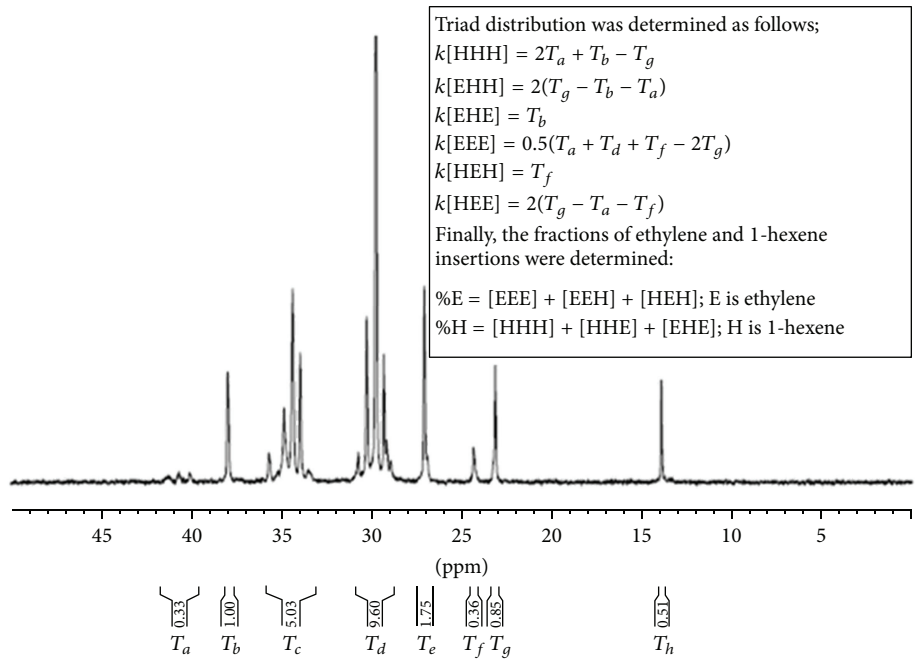

Figure 7: A typical ^{13}CNMR spectrum of LLDPE.

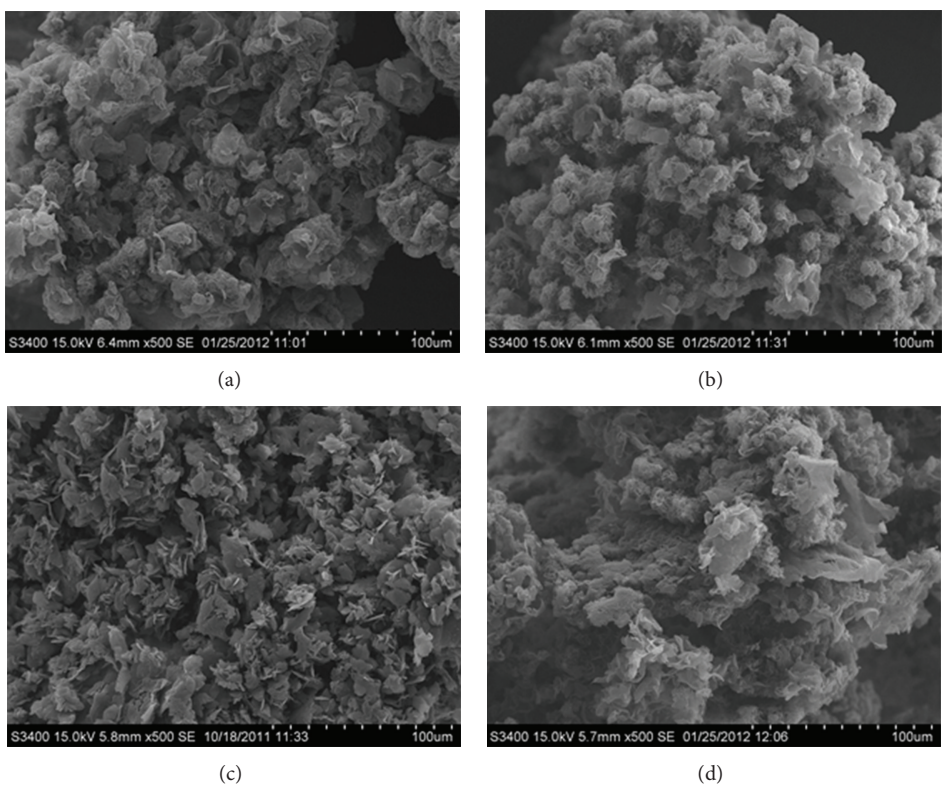

(a) (b)

(c) (d)

Figure 8: SEM images of PE samples. (a) PE, (b) PE/clay 5, (c) PE/clay 10, and (d) PE/clay 20.

of the clays, which reduces a tendency for the clays to agglomerate. In addition, the strong interaction between the clay surface and the polymer matrix may help reduce the leaching of the clays. These advantages would come from the *in situ* polymerization, in which the catalyst covalently bound between the clay layers becomes the reaction center during the polymerization and was attacked and linked with the monomer; therefore, the strong interaction between

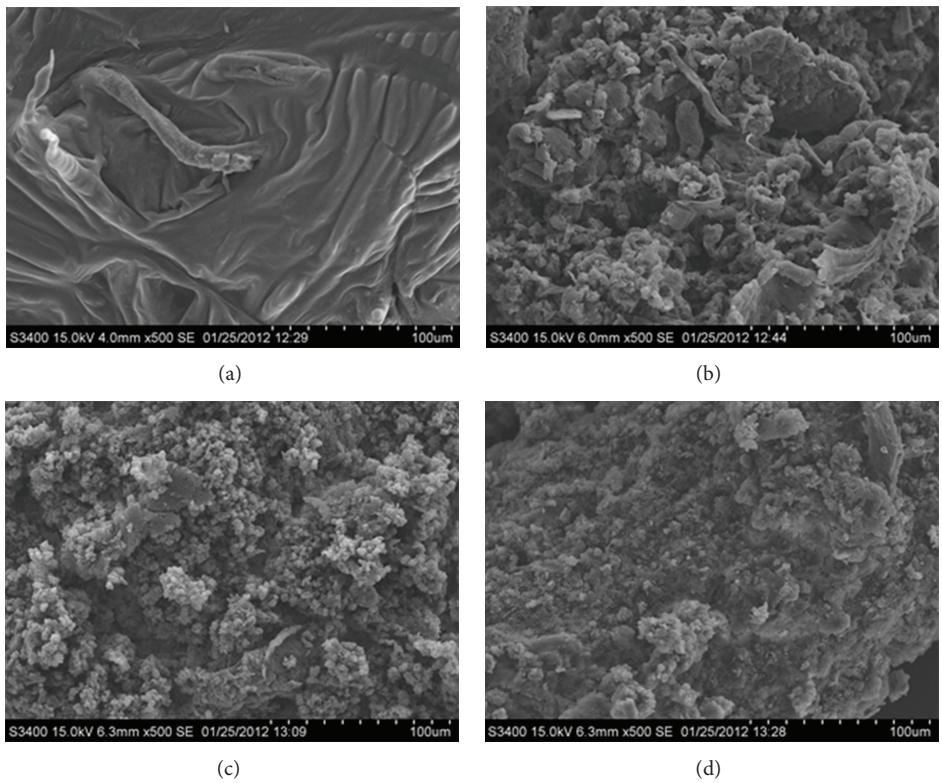

(a) (b) (c) (d)

Figure 9: SEM images of LLDPE samples. (a) LLDPE, (b) LLDPE/clay 5, (c) LLDPE/clay 10, and (d) LLDPE/clay 20.

the clay and the polymer occurred. Moreover, when the polymer had been propagating it exfoliated the clay layers all over the polymer matrix, with the good distribution of the clays being obtained [22]. The morphologies of all PE/clay nanocomposites did not change upon various clay contents. This suggests that the good distribution of clay still occurs even the high clay content. From Figure 9, it is observed that the morphology of pure LLDPE differed considerably from the entire LLDPE/clay nanocomposites. The presence of clays improved greatly the morphology of LLDPE by providing the pellet-like structure, which is required for the polymer processing. The variation of clay content did not significantly affect the morphologies of LLDPE/clay nanocomposites.

4. Conclusions

The *in situ* polymerization in which catalyst was first immobilized onto the nanoclay, and then brought the nanoclays/catalyst into the polymerization process, appeared to be a good method for producing polymer nanocomposites with an excellent distribution of the nanoclays inside the polymer matrix. The distribution of the nanoclays can be proven by X-ray diffraction analysis (XRD), which no peak indicating to the nanoclays was observed suggesting high dispersion of nanoclay throughout the polymer matrix. Both clay A and clay B can improve thermal stability for the host polymers. However, clay B provided the lower catalytic activity to the polymerization system than clay A due to the higher amount of amine group, which could deactivate the catalyst. The clay content adversely affected the catalytic activity for both PE and LLDPE and also affected the comonomer insertion in the case of LLPDE.

Acknowledgment

The authors thank "The Ratchadaphiseksomphot Endowment Fund of Chulalongkorn University (RES5605300086-AM)".

References

[1] O. G. Piringer and A. L. Baner, *Plastic Packaging: Interactions with Food and Pharmaceuticals*, Wiley-VCH, 2nd edition, 2008.

[2] L. Chen, R. Ozisik, and L. S. Schadler, "The influence of carbon nanotube aspect ratio on the foam morphology of MWNT/PMMA nanocomposite foams," *Polymer*, vol. 51, no. 11, pp. 2368–2375, 2010.

[3] D. Zhang and T. Cui, "Tunable mechanical properties of layer-by-layer self-assembled carbon nanotube/polymer nanocomposite membranes for M/NEMS," *Sensors and Actuators A*, vol. 185, pp. 101–108, 2012.

[4] S. Barus, M. Zanetti, M. Lazzari, and L. Costa, "Preparation of polymeric hybrid nanocomposites based on PE and nanosilica," *Polymer*, vol. 50, no. 12, pp. 2595–2600, 2009.

[5] X. Huang, Z. Ma, Y. Wang, P. Jiang, Y. Yin, and Z. Li, "Polyethylene/aluminum nanocomposites: improvement of dielectric strength by nanoparticle surface modification," *Journal of Applied Polymer Science*, vol. 113, no. 6, pp. 3577–3584, 2009.

[6] C. Zhao, H. Qin, F. Gong, M. Feng, S. Zhang, and M. Yang, "Mechanical, thermal and flammability properties of polyethylene/clay nanocomposites," *Polymer Degradation and Stability*, vol. 87, no. 1, pp. 183–189, 2005.

[7] G. Huang, B. Zhu, and H. Shi, "Combination effect of organics-modified montmorillonite with intumescent flame retardants on thermal stability and fire behavior of polyethylene nanocomposites," *Journal of Applied Polymer Science*, vol. 121, no. 3, pp. 1285–1291, 2011.

[8] P. Meneghetti and S. Qutubuddin, "Synthesis, thermal properties and applications of polymer-clay nanocomposites," *Thermochimica Acta*, vol. 442, no. 1-2, pp. 74–77, 2006.

[9] S. Hakim, M. Safajou-Jahankhanemlou, and M. Zeynali, "Polyethylene nanocomposite prepared by a metallocene catalyst supported on MMT using a new pretreatment method," *Journal of Polymer Research*, vol. 20, no. 5, pp. 1–10, 2013.

[10] P. Zapata, R. Quijada, C. Covarrubias, E. Moncada, and J. Retuert, "Catalytic activity during the preparation of PE/clay nanocomposites by in situ polymerization with metallocene catalysts," *Journal of Applied Polymer Science*, vol. 113, no. 4, pp. 2368–2377, 2009.

[11] S. O. Vilela, M. A. Soto-Oviedo, A. P. F. Albers, and R. Faez, "Polyaniline and mineral clay-based conductive composites," *Materials Research*, vol. 10, no. 3, pp. 297–300, 2007.

[12] R. M. Silverstein, G. C. Bassler, and T. C. Morrill, *Spectrometric Identification of Organic Compounds*, John Wiley and Sons, New York, NY, USA, 1981.

[13] F. Dietsche, Y. Thomann, R. Thomann, and R. Mülhaupt, "Translucent acrylic nanocomposites containing anisotropic laminated nanoparticles derived from intercalated layered silicates," *Journal of Applied Polymer Science*, vol. 75, no. 3, pp. 396–405, 2000.

[14] S. K. Ackerman, A. K. Agapiou, M. L. DeChellis, and D. M. LaBorde, *Process for Deactivating Ziegler-Natta and Metallocene Catalysts*, Exxon Chemical Patents, 1994.

[15] F. Silveira, G. P. Pires, C. F. Petry et al., "Effect of the silica texture on grafting metallocene catalysts," *Journal of Molecular Catalysis A*, vol. 265, no. 1-2, pp. 167–176, 2007.

[16] Y. H. Lee, T. Kuboki, C. B. Park, M. Sain, and M. Kontopoulou, "The effects of clay dispersion on the mechanical, physical, and flame-retarding properties of wood fiber/polyethylene/clay nanocomposites," *Journal of Applied Polymer Science*, vol. 118, no. 1, pp. 452–461, 2010.

[17] Y. Choi and J. B. P. Soares, "Supported single-site catalysts for slurry and gas-phase olefin polymerisation," *Canadian Journal of Chemical Engineering*, vol. 90, no. 3, pp. 646–671, 2012.

[18] X. Wang, T. T. Fangfang, X. Gi et al., "Enhanced exfoliation of organoclay in partially end-Functionalized non-polar polymer," *Macromolecular Materials and Engineering*, vol. 294, no. 3, pp. 190–195, 2009.

[19] S. M. Lomakin, L. A. Novokshonova, P. N. Brevnov, and A. N. Shchegolikhin, "Thermal properties of polyethylene/montmorillonite nanocomposites prepared by intercalative polymerization," *Journal of Materials Science*, vol. 43, no. 4, pp. 1340–1353, 2008.

[20] M. Zanetti, P. Bracco, and L. Costa, "Thermal degradation behaviour of PE/clay nanocomposites," *Polymer Degradation and Stability*, vol. 85, no. 1, pp. 657–665, 2004.

[21] G. Leone, F. Bertini, M. Canetti, L. Boggioni, P. Stagnaro, and I. Tritto, "In situ polymerization of ethylene using metallocene catalysts: effect of clay pretreatment on the properties of highly filled polyethylene nanocomposites," *Journal of Polymer Science A*, vol. 46, no. 16, pp. 5390–5403, 2008.

[22] S.-Y. A. Shin, L. C. Simon, J. B. P. Soares, and G. Scholz, "Polyethylene-clay hybrid nanocomposites: in situ polymerization using bifunctional organic modifiers," *Polymer*, vol. 44, no. 18, pp. 5317–5321, 2003.